

AdaptGOT: A Pre-trained Model for Adaptive Contextual POI Representation Learning

Xiaobin Ren
University of Auckland
Auckland, New Zealand
xren451@aucklanduni.ac.nz

Xinyu Zhu
University of Auckland
Auckland, New Zealand
xzhu662@aucklanduni.ac.nz

Kaiqi Zhao
University of Auckland
Auckland, New Zealand
kaiqi.zhao@auckland.ac.nz

Abstract

Currently, considerable strides have been achieved in Point-of-Interest (POI) embedding methodologies, driven by the emergence of novel POI tasks like recommendation and classification. Despite the success of task-specific, end-to-end models in POI embedding, several challenges remain. These include the need for more effective multi-context sampling strategies, insufficient exploration of multiple POI contexts, limited versatility, and inadequate generalization. To address these issues, we propose the **AdaptGOT** model, which integrates both the (**Adapt**)ive representation learning technique and the Geographical-Co-Occurrence-Text (**GOT**) representation with a particular emphasis on Geographical location, Co-Occurrence and Textual information. The **AdaptGOT** model comprises three key components: (1) **contextual neighborhood generation**, which integrates advanced mixed sampling techniques such as KNN, density-based, importance-based, and category-aware strategies to capture complex contextual neighborhoods; (2) an advanced **GOT representation** enhanced by an attention mechanism, designed to derive high-quality, customized representations and efficiently capture complex interrelations between POIs; and (3) the **MoE-based adaptive encoder-decoder** architecture, which ensures topological consistency and enriches contextual representation by minimizing Jensen-Shannon divergence across varying contexts. Experiments on two real-world datasets and multiple POI tasks substantiate the superior performance of the proposed AdaptGOT model.

ACM Reference Format:

Xiaobin Ren, Xinyu Zhu, and Kaiqi Zhao. 2018. AdaptGOT: A Pre-trained Model for Adaptive Contextual POI Representation Learning. In *Proceedings of Make sure to enter the correct conference title from your rights confirmation email (Conference acronym 'XX)*. ACM, New York, NY, USA, 11 pages. <https://doi.org/XXXXXXX.XXXXXXX>

1 Introduction

The recent progressions in location-based systems have enabled users to share their experiences and insights at points of interest (POIs). The accumulation and accessibility of significant footprint data serve as the foundation for advancing POI recommendations,

Permission to make digital or hard copies of all or part of this work for personal or classroom use is granted without fee provided that copies are not made or distributed for profit or commercial advantage and that copies bear this notice and the full citation on the first page. Copyrights for components of this work owned by others than the author(s) must be honored. Abstracting with credit is permitted. To copy otherwise, or republish, to post on servers or to redistribute to lists, requires prior specific permission and/or a fee. Request permissions from permissions@acm.org.
Conference acronym 'XX, June 03–05, 2018, Woodstock, NY

© 2018 Copyright held by the owner/author(s). Publication rights licensed to ACM.
ACM ISBN 978-1-4503-XXXX-X/2018/06...\$15.00
<https://doi.org/XXXXXXX.XXXXXXX>

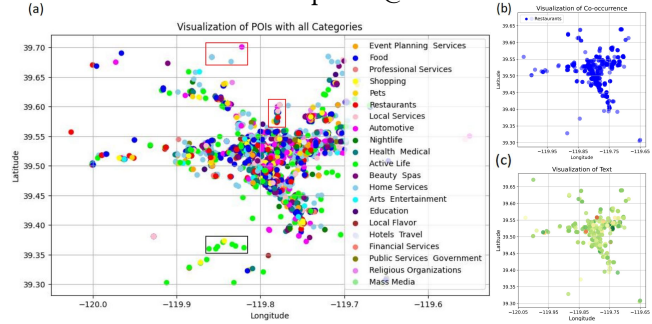


Figure 1: (a) Visualization of POIs on Yelp Nevada dataset. (b) Co-occurrence of all POIs, darker blue indicates frequent co-selection with other POIs. (c) Sentiment analysis of all POIs, with orange representing negative evaluations.

category classification, function zone identification, and the discernment of users' living patterns [23, 26], etc. In this context, significant attention has been directed toward investigating POI embedding, aiming to capture intricate semantic relationships and contextual information associated with POIs to enhance diverse location-based applications and analysis.

POI embedding plays a pivotal role in various downstream tasks. A wide range of contextual information has been considered in POI embedding, such as geographical coordinates, POI sequences, spatial co-occurrence patterns of POIs, textual information, and additional auxiliary features. POI2Vec [12] and Hier-CEM [6] leverage geographical coordinates to embed spatially organised POI pairs, modelling complex spatial correlations for category prediction tasks. Similarly, HMRM [5] and GeoSAN [23] utilise user trajectory data to capture POI co-occurrences. Besides, recent work [46] incorporates contextual information through an additional content layer to integrate textual data.

Despite the notable achievements of contemporary methodologies, several limitations warrant further investigation.

First, current research lacks consideration of diverse sampling strategies under multiple POI contexts (Gap 1). Existing POI-based graph models fall into three categories: Expressive Graph Neural Networks (GNNs)[29, 30], Message Passing Neural Networks (MPNN)[16, 25], and subgraph-based approaches [17]. While more expressive k-WL GNNs [30] address this limitation, their reliance on $O(k)$ -order tensors restricts scalability for large graphs. Recent studies have explored subgraph sampling to balance expressive power and scalability [40, 48], yet the integration of multiple contexts remains limited, introducing randomness in sampled graphs [17, 43, 51]. Importantly, leveraging multiple subgraphs has been shown to match the expressive power of MPNNs when using sufficient layers and injective functions [38, 49]. Therefore,

current POI representation frameworks fail to fully exploit multi-subgraph approaches under multi-context scenarios [2, 9], risking over-smoothing in the embedding space [47]. Incorporating diverse contexts mitigates this issue and enhances model robustness.

Second, there is a lack of comprehensive investigations of multiple POI contexts simultaneously (Gap 2). Existing research predominantly focuses on specific contexts, such as geographical locations, categories, co-occurrence, or textual information. However, none of the current methods fully integrate these POI contexts, limiting their broader applicability. As illustrated in Figure 1(a), geographical location demonstrates diverse spatial correlations with categories, with certain areas exhibiting a higher density of various categories. Additionally, Figures 1(b) and (c) highlight the distinct correlations of co-occurrence and textual information with geographical location. These intricate interrelations necessitate a comprehensive and holistic investigation of multiple POI contexts simultaneously.

Third, fixed pre-trained POI embeddings encounter significant limitations when applied to diverse downstream tasks (Gap 3). For instance, the task of POI categorization requires an analysis of spatially proximate POIs, whereas the next POI recommendation might prioritize POIs that are visited within a short time frame [21]. However, the fixed pre-trained POI embeddings generated by existing methods lack the flexibility to adapt effectively to tasks that demand distinct contextual information.

To address the aforementioned challenges, we introduce Adapt-GOT, which builds upon a pre-trained adaptive representation model through Mixture-of-Expert (MoE) with the integration of Geographical-Co-Occurrence-Text (GOT) representations. To address **Gap 1**, we propose a **mixed sampling subgraphs** considering multiple contexts and diverse POI neighborhoods. This design can naturally encode the locally induced subgraphs and will uplift the base model of modified GATs. The mixed sampling scheme based on several subgraphs will generate new node embeddings to overcome the over-smoothing (Section 5.4) and boost the expressive power theoretically. To address **Gap 2**, we propose a **GOT representation module** to acquire three predominant representations: co-occurrence, geographical, and texts. These representations are further transformed in the **GOT attention module**, which generates the latent node and neighborhood representations in an inductive manner. To address **Gap 3**, we propose a specialised **adaptive encoder-decoder framework** featuring an MoE-based mechanism that dynamically adjusts POI representations across tasks without retraining. This is achieved by minimising the Jensen-Shannon (JS) divergence between sampled subgraph and raw graph distributions. The **adaptive representation aggregator** maintains subgraph topological integrity while enhancing contextual expressiveness, thereby facilitating multi-contexts decoding across POI tasks.

We summarize the contributions of this research as follows:

- **Mixed Subgraph Sampling Scheme:** The mixed sampling strategy integrates multiple contexts and diverse POI neighborhoods. This approach encodes locally induced subgraphs and enhances the expressive power of the base model (modified GATs) by generating new node embeddings from multiple subgraphs.

- **GOT Representation and GOT Attention Module:** The GOT representation module captures three key aspects of POI data: co-occurrence, geographical, and texts. These representations are further processed using a GOT attention module to generate latent node and neighborhood embeddings in an inductive manner.
- **Adaptive Encoder-Decoder Architecture:** This architecture effectively selects diverse contextual neighborhoods while preserving the topological consistency of subgraphs through the minimization of Jensen-Shannon (JS) divergence, enhancing the contextual and structural representation capabilities.

2 Related Work

2.1 POI Contextual Learning

Recent advancements in recommender systems have focused on enhancing POI embeddings by integrating diverse contextual factors, including geographical, textual, and spatio-temporal information [2, 5, 23]. Approaches such as hierarchical encoders, text-based context layers, and trajectory modeling highlight the importance of multi-contextual integration in improving POI representations [9, 26, 41].

To improve the generalizability of POI embeddings, new studies have explored pre-training techniques. For example, MGeo [11] has pioneered a pre-trained POI embedding technique that integrates geographic context to extract multi-modal correlations crucial for precise query-POI matching. CTLE [24] devises a pre-trained method that computes a location’s representation vector by considering its specific contextual neighbors within trajectories. SpaBERT [22] offers a versatile geo-entity representation based on neighboring entities in geospatial datasets. However, CTLE bias towards the next POI recommendation task. While SpaBERT demonstrates generalizability to cross-city tasks, it produces a fixed POI embedding, which inevitably impacts the model’s accuracy and effectiveness in diverse tasks emphasizing distinct contexts. More recently, M3PT was proposed as a contextual POI learning framework. While its fusion of textual and visual features achieves promising results, its heavy reliance on image modality and lack of sequential modelling limit its generalisability and practical utility [39].

2.2 Sampling models

In the realm of sampling, it has been well acknowledged that the application of Graph Neural Networks (GNNs) to large-scale graphs presents considerable challenges due to the substantial computational and memory costs associated with the training process [43]. As a result, numerous researchers have undertaken efforts to develop simplified models aimed at expediting the training process. These models can be broadly categorized into three main types: node-wise sampling [8][4][43], layer-wise sampling [3][51][15], and subgraph sampling [7][45]. In node-wise sampling, a set of neighbors is sampled for each node. Layer-wise sampling involves selecting layer-dependent neighbors based on the calculation of importance for different nodes. While each method has demonstrated efficiency in sampling, they lack the ability to integrate different graph topologies effectively. Furthermore, in the context of POI, existing research fails to determine appropriate graph topologies when considering multiple POI contexts [41].

3 Problem Definition & Theoretical Analysis

3.1 Problem definition

Let $P = \{p_1, p_2, p_3, \dots, p_N\}$ be a set of POIs, $U = \{u_1, u_2, u_3, \dots, u_M\}$ denote a set of users and $T = \{t_1, t_2, t_3, \dots, t_K\}$ signify a set of timesteps, where N, M, K denote the positive integers. Each POI $p \in P$ is characterized by a tuple $p = \langle lat, lon, cat \rangle$ comprising latitude, longitude, and category. A check-in is defined as a tuple $q = \langle u, p, t \rangle \in U \times P \times T$, indicating that users u visit p at timestep t . We denote the set of all check-ins by Q . Let X_{u_i, p_j}^{txt} denote the review texts from user i pertaining to POI p_j , where i represents the i -th user and j represents the j -th POI. The objective of AdaptGOT is to generate pre-trained embeddings $H = f(X_{U, P}^{txt}, P, Q)$ for all POIs following the self-supervised manner.

3.2 Expressive power analysis

Existing studies have proved the effectiveness of the graph formulation of POI data in learning POI representations [47][44]. Following prior work [50], we construct a POI graph $G = (\mathcal{V}, \mathcal{E})$ where each node in \mathcal{V} is a POI, and the edges in \mathcal{E} are learnable and determined by the node features. However, as discussed in Section 1, existing MPNNs and subgraph-based models may not be adequate for learning robust and effective POI representations. To obtain a theoretical view of the problem, we will first analyze the bottleneck at current MPNNs and subgraph-based methods. Subsequently, we will theoretically justify the need for mixed sampling strategies to improve the expressiveness of the learned embedding.

3.2.1 MPNNs Let $h_{p_i}^l$ denotes the embedding of p_i , then the MPNNs can be described as follows:

$$\begin{aligned} h_{p_i}^{(l+1)} &= \phi^{(l)} \left(h_{p_i}^{(l)}, f^{(l)} \left(h_{p_j}^{(l)} \mid u \in \mathcal{N}(v) \right) \right); l = 0, \dots, L - 1; \quad (1) \\ h_G &= \text{POOL} \left(H_v^l \mid v \in \mathcal{V} \right), \quad (2) \end{aligned}$$

where $h_{p_i}^{(0)} = x_i$ is the constructed feature vector of POI p_i , ϕ represents the injective function. The expressive power of MPNNs' upper bound from its close relation to the 1-WL isomorphism test [29]. Note that the current MPNNs rely heavily on the star graph with limited features, which makes the star not distinguishing enough [49]. In view of that, the design of the subgraph under multiple contexts will facilitate the isomorphism test.

3.2.2 1-WL isomorphism test The 1-WL is a widely used framework in graph theory to determine the equivalence of two graphs by iteratively updating node embeddings based on local neighborhood information. The node embeddings at iteration $t + 1$ are updated as:

$$h_v^{(t+1)} = \text{Hash} \left(h_v^{(t)}, \text{multiset} \{ h_u^{(t)} : u \in \mathcal{N}(v) \} \right) \quad (3)$$

The process begins with initial attributes $h_v^{(0)}$, which typically represents node attributes or graph-invariant properties such as degree. Hash() denotes the Hash function.

3.2.3 Multiple contexts Next, we demonstrate that using multiple contexts enhances expressive power through Theorems 1 and 2. Theorem 1 shows that multiple contexts reduce feature duplication, improving the 1-WL test's discriminative power. Theorem 2

proves that integrating multiple contexts increases node embedding entropy. Figure 2 (d) illustrates these findings by an example.

Theorem 1¹: *Incorporating multiple contexts reduces the probability of feature duplication among nodes, thereby enhancing the discriminative power of the 1-WL test. Specifically,*

$$P_{\text{conflict}}^{\text{single}} \geq P_{\text{conflict}}^{\text{multi}}, \quad (4)$$

where $P_{\text{conflict}}^{\text{single}}$ and $P_{\text{conflict}}^{\text{multi}}$ represent the probabilities of feature conflict between two distinct nodes in single-feature graphs and multi-feature graphs, respectively.

We provide the proof by analyzing the feature space size in multiple-feature case grows exponentially with dimension size k , significantly reducing the likelihood of conflicts. The (1) and (2) of Figure 2 (d) also support our claim. Utilizing additional feature will generate discriminative label $X(\tilde{G}, 1)$ through the first update. However, using one feature will bring duplicated labels.

Theorem 2. *Incorporating POI contextual information into node representations increases the entropy of the node embedding.*

$$H(\tilde{G}) \geq H(G), \quad (5)$$

where $H(\tilde{G})$ represents the entropy under multiple features.

We prove Theorem 2 by comparing entropy before and after incorporating additional features. As shown in Figure 2 (d), the entropy increases from $H(G) = 1$ to $H(\tilde{G}) = 2$.

3.2.4 Subgraphs under multiple contexts To mitigate the problems of existing subgraph-based methods, we propose to leverage multiple contexts of POIs. As a result, the node features can be enriched by these contexts. Next, we will then introduce why enriching node features enhances expressive power by 1-WL isomorphism test.

Theorem 3. *Leveraging multiple subgraphs enhances entropy and improves label discrimination.*

The entropy of the node label distribution after the t -th update in the 1-WL test satisfies:

$$P_{\text{multi}}^{(t)} \geq P_{\text{single}}^{(t)}, H_{\text{multi}}^{(t)} \geq H_{\text{single}}^{(t)}. \quad (6)$$

where $P_{\text{single}}^{(t)}$ and $H_{\text{single}}^{(t)}$ stands for the entropy and probability of the label conflict of a single graph, while $P_{\text{multi}}^{(t)}$ and $H_{\text{multi}}^{(t)}$ represent the entropy and label conflict of multiple subgraphs. The proof follows the similar process of Theorem 1 and 2. Also, we conclude that the entropy $H(\tilde{G}_g) = 2.58$ in Figure 2 (d) for subgraphs G_g under single feature and multiple features, which shows that applying multiple subgraphs will bring better representative power.

4 Methodology

In this work, we propose AdaptGOT, a unified framework for POI representation learning that addresses three key challenges: the need for scalable context-aware sampling, unified multi-context POI representations, and adaptive subgraph selection for POI tasks. AdaptGOT comprises three core components. First, a mixed subgraph sampling strategy integrates diverse POI contexts to enhance expressive power. Second, the GOT representation and attention module unifies three POI contexts, while its attention mechanism inductively generates latent node and neighborhood embeddings.

¹Detailed proof on Theorem 1, 2, and 3: <https://anonymous.4open.science/r/AdaptGOT-2748/README.md>

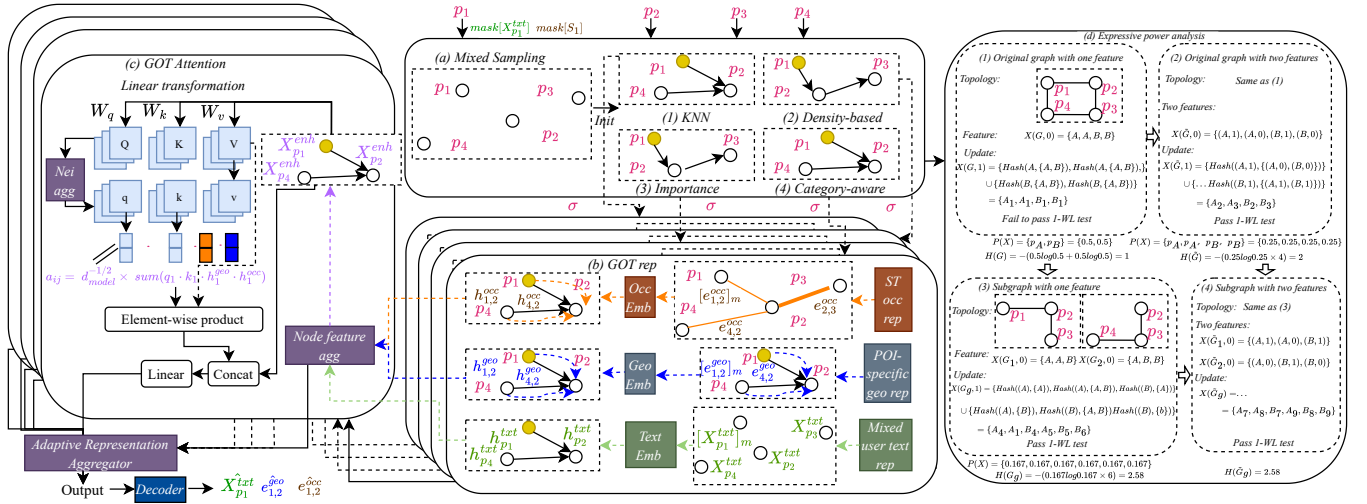


Figure 2: Architecture (a), (b), (c) and expressive power (d) of AdaptGOT. In (d), we initialize one or two features across different graph topologies to demonstrate the 1-WL test and examine the entropy under each scenario on Section 3.2.

Finally, the architecture adaptively selects contextual neighborhoods and preserves topological consistency through JS divergence minimization, improving structural and contextual representations. Figure 2 shows the architecture of AdaptGOT.

4.1 Contextual Neighborhood Identification via Mixed Sampling

To effectively capture diverse POI contextual information, we propose a comprehensive sampling scheme incorporating four strategies. KNN and density-based sampling address geographical proximity, with KNN focusing on local neighbors and density-aware sampling capturing broader spatial correlations. Importance sampling leverages GOT contexts to prioritize significant POI interactions, while category-aware sampling considers categorical similarities. Notably, this is the first work to introduce multiple sampling schemes for POI embeddings considering multiple contexts.

4.1.1 KNN sampling The KNN sampling method selects a fixed number k of the nearest neighbors $\mathcal{N}_{knn}(p_i)$ for a given POI p_i , based on geographical proximity. Here, \mathcal{N}_{knn} denotes the set of neighboring POIs identified by the KNN algorithm.

4.1.2 Density-based sampling To account for the visiting preferences of different users towards specific p_i , we calculate the density across all historical moments T and then identify the top- k neighbors. Formally, this can be expressed as:

$$\mathcal{N}_{den}(p_i) = \text{Topk}(\text{Den}(p_i, g(p_i))), \quad (7)$$

where \mathcal{N}_{den} denotes the density-based neighboring set, g function returns the correlated historical check-in of p_i , and Den represents the density function, which is defined as:

$$\hat{\text{Den}}(\mathbf{x}) = \frac{1}{|\mathcal{N}_{den}|b^2} \sum_{n=1}^{|\mathcal{N}_{den}|} K\left(\frac{p' - p'_n}{b}\right), \quad (8)$$

where p'_n represents the subset of p that includes only the latitude and longitude on the n -th POI, b denotes the bandwidth and K denotes the non-parametric Gaussian kernel [13].

4.1.3 Importance sampling The importance sampling has been studied by many works [3, 51] while complicated POI contexts are neglected, like positive remarks of reviews. Our importance sampling method aggregates textual information $X_{p_i}^{txt}$, the frequency matrix $X_{p_i}^{freq}$, and the distance matrix D_{u_i} . It is defined as:

$$\mathcal{N}_{imp}(p_i) = \text{Topk}\left(\frac{X_{p_i}^{freq} \odot \text{Senti}(X_{*p_i}^{txt}) + \gamma}{D_{u_i} + \gamma}\right), \quad (9)$$

where $X_{p_i}^{freq}$ represents the frequency matrix of all users in p_i , $X_{*p_i}^{txt}$ represents the set of reviews from all users regarding POI p_i , and Senti denotes the sentiment analysis function, which returns a positive, negative, or neutral evaluation of a review by analyzing the frequency of various words [27], as illustrated in Figure 1(c). The symbol \odot indicates the element-wise product and a small value γ is added to prevent zero denominators.

4.1.4 Category-aware sampling Category-aware sampling strategy bears resemblance to the approach delineated in Equation (9). Formally, this strategy is formulated as follows:

$$\mathcal{N}_{cat}(p_i) = \text{Topk}\left(\frac{X_{u_i}^{freq} \odot X_{u_i}^{cat} + \gamma}{D_{u_i} + \gamma}\right), \quad (10)$$

where $X_{u_i}^{cat}$ denotes the category-based matrix, which computes the normalized frequency matrix of the category.

4.2 GOT representation

After capturing comprehensive contextual neighborhoods using the mixed sampling scheme, the GOT representation is proposed to create a unified representation that fully captures the intricate interrelationships among location, co-occurrence, and category information simultaneously.

4.2.1 Spatio-temporal Co-occurrence representation We selected co-occurrence as one of the POI contexts because it can be combined with historical POIs to measure general user preferences over a long time span. Additionally, it eliminates the need for time encoding in models like transformers, making the model suitable for zero-shot cross-city scenarios (Experiment on Section 5.6).

Giving S_i as the complete set of historical check-ins for i -th users over timesteps T , the co-occurrence representation can be formulated as :

$$O_{i,j} = \frac{\#Occ_{i,j}}{\#S_i}, \quad (11)$$

where $\#Occ_{i,j}$ stands for the number of co-occurrence between p_i and p_j , S_i serve to normalize the co-occurrence $Occ_{i,j}$ to obtain normalized co-occurrence $O_{i,j}$.

4.2.2 POI-specific Geographical representation and embedding Unlike SpaBERT[22], we design a POI-specific geographical representation that integrates a relative position encoding. Specifically, given a pair of POIs p_i, p_j , the relative position of two POIs is captured using the following equations: $r_{ij} = [s, \theta_1]$, $r_{ji} = [s, \theta_2]$, where s represents the distance, and θ_1 and θ_2 denote the azimuth from p_i to p_j and from p_j to p_i respectively.

With the relative position vectors r_{ij} , we employ a two-layer FCN to obtain the geographical representation of a POI p_i given its geographical neighbor p_j :

$$c_{ij} = (r_{ij}W_r^1 + b_r^1)W_r^2 + b_r^2, c_{ij} \in \mathbb{R}^{d_{model}}, \quad (12)$$

where W_r^1, W_r^2, b_r^1 and b_r^2 are learnable parameters.

4.2.3 Mixed user text representation We formulate a composite user text representation alongside a BERT text embedding [10] to effectively capture textual information. Since each POI receives a range of reviews, both positive and negative, from different users, we aggregate all users' reviews for each POI separately to form a unified evaluation of the POI. Formally, X_{p_i, u_j}^{txt} represents the review of user j towards the i -th POI.

$$X_{p_i}^{txt} = \text{Concat}\{X_{p_i, u_1}^{txt}, X_{p_i, u_2}^{txt}, \dots, X_{p_i, u_M}^{txt}\} \quad (13)$$

where $X_{p_i}^{txt}$ denotes the representation of each POI across all users with regard to integrated textual information.

4.2.4 Text embedding We adopt a $BERT_{base}$ as the encoder of text embedding to reflect the sophisticated sentiment, preference and descriptive nuances articulated by the user community. The equation on text embedding $h_{p_i}^{txt}$ can be written as follows:

$$h_{p_i}^{txt} = BERT_{encoder}(X_{p_i}^{txt}) \quad (14)$$

4.3 GOT Attention

The GOT representation module produces unified representations, which the GOT attention mechanism integrates using a POI feature aggregator (Figure 2). Node features Q, K , and V are updated to q, k , and v , enabling information aggregation from neighbors. The modified self-attention mechanism uses the dot-product of q, k , h^{occ} , and h^{geo} to model pairwise relationships by incorporating spatial positions and co-occurrence. The final output z_i is obtained via element-wise product, concatenation, and linear transformation.

4.3.1 Node feature aggregation The geographical embeddings $h_{1,2}^{geo}$ and co-occurrence embeddings $h_{1,2}^{occ}$ are depicted by the edge from the first p_1 to the second p_2 within the GNNs, while the textual embeddings $h_{p_1}^{txt}$ and $h_{p_2}^{txt}$ serve as the node features for p_1 and p_2 respectively. For p_1 , the aggregation of its node features involves summing geographical representations h^{geo} , co-occurrence representations h^{occ} , and the inherent textual representations h^{txt} across all its neighbors. This aggregation is expressed as equation 15:

$$X_{p_1}^{enh} = \text{Concat} \left(\sum (h_{1,2}^{geo}, h_{1,3}^{geo}, \dots, h_{1, n_{geo}}^{geo}), \sum (h_{1,2}^{occ}, h_{1,3}^{occ}, \dots, h_{1, n_{occ}}^{occ}), h_{p_1}^{txt} \right), \quad (15)$$

where $X_{p_1}^{enh}$ denotes the enhanced feature of p_1 after amalgamating textual, geographical, and co-occurrence information. n_{geo} and n_{occ} represent the number of geographical entities and co-occurrence entities in the aggregation, respectively, equivalent to the number of neighbors as predefined.

4.3.2 Neighboring feature aggregation Let $X_p^{enh} = [X_{p_i: p_n}^{enh}]$ denote the input embeddings for all nodes after feature aggregation. Neighboring feature aggregation involves transforming X_p^{enh} into query, key, and value matrices (Q, K, V) and further indexing them based on edge connectivity to produce edge-specific representations (q, k, v):

$$Q = X_p^{enh}W^Q, \quad K = X_p^{enh}W^K, \quad V = X_p^{enh}W^V, \\ q = Q[\text{edge}[0, :]], \quad k = K[\text{edge}[1, :]], \quad v = V[\text{edge}[1, :]], \quad (16)$$

where W^Q, W^K , and W^V are learnable parameter matrices. The edge-level transformation enables the model to prioritize information flow between connected nodes, effectively integrating node features and edge attributes to capture local graph structures.

4.3.3 Modified attention mechanism We propose a relative position encoder to simultaneously include both geographical and co-occurrence embeddings. It is designed to compute the output z_i for the i -th POI by integrating geographical and co-occurrence contexts into the attention scores, as expressed by Equation 17:

$$z_i = \sum_{j=1}^n \alpha_{ij} v_j \in \mathbb{R}^{d_k}, \quad \alpha_{ij} = \frac{\exp(e_{ij})}{\sum_{k=1}^n \exp(e_{ik})}, \\ e_{ij} = \frac{\text{sum}(q_i \odot k_j \odot h_{ij}^{geo} \odot h_{ij}^{occ})}{\sqrt{d_k}}, \quad (17)$$

where α_{ij} represents the normalized weight using a softmax function, and e_{ij} denotes the attention score from node j to i .

Subsequently, we concatenate all outputs from different heads through a projection operation, which consolidates and refines the information captured by each head into a cohesive representation, as demonstrated in the equation below:

$$Z_i = \text{Concat}(z_i^{(1)}, z_i^{(2)}, \dots, z_i^{(h)})W^O, \quad (18)$$

where W^O is the parameter matrix for linear transformation and $z_i^{(h)}$ is the output of the h -th head.

Furthermore, to enhance the model's generalization capabilities and mitigate overfitting, we apply normalization and dropout

techniques to this projected representation to generate the final representation z_i^{final} .

$$z_i^{final} = \text{Droupout}(\text{LayerNorm}(Z_i)) \quad (19)$$

4.4 Adaptive Representation Aggregator

Following the aggregation of neighborhoods using the GOT attention mechanism, the adaptive representation aggregator is applied to dynamically select the expert associated with each contextual graph motivated by MoE [28]. Unlike existing pre-trained model that produces a fixed representation for each POI [22], the adaptive representation learning technique can dynamically adjust the representation to different tasks without retraining. The subgraph representations can be further minimized by Jensen-Shannon (JS) divergence on subgraphs and original graphs. The structure can be delineated by:

$$h'_i = \sigma \left(\sum_{o=1}^4 G \left(X_{p_i}^{enh} \right)_o \cdot z_{i,o}^{final} \right), \quad (20)$$

$$Q(z_{i,o}^{final}) = W_g \cdot z_{i,o}^{final} + \epsilon \cdot \text{Softplus}(z_{i,o}^{final} \cdot W_n), \quad (21)$$

$$G(h_i) = \text{softmax}(\text{Topk}(Q(z_{i,o}^{final}))), \quad (22)$$

where h'_i represents the latent representation of MoE, o denotes the o -th expert, $G \left(X_{p_i}^{enh} \right)_o$ stands for the gating weights for expert o , and $\epsilon \in \mathcal{N}(0, 1)$ is the standard Gaussian noise. $W_g \in \mathbb{R}^{s \times n}$ and $W_n \in \mathbb{R}^{s \times n}$ are learnable weights that determine the clean and noisy scores, respectively. Finally, $G(h_i)$ produces a sparse probability distribution over experts, decides how strongly each expert's output contributes to the framework.

In addition to dynamically assigning experts to contextual subgraphs, the adaptive representation aggregator refines subgraph topology by minimising the JS divergence between subgraph and original graph feature distributions, thereby preserving global structural fidelity. The JS divergence is defined as:

$$D_{\text{JS}}(P(G_s) \| P(G)) = \frac{1}{2} D_{\text{KL}}(P(G_s) \| M) + \frac{1}{2} D_{\text{KL}}(P(G) \| M), \quad (23)$$

where $M = \frac{1}{2}(P(G_s) + P(G))$ is the midpoint distribution in equation 23, and D_{KL} is the Kullback-Leibler divergence.

The context-specific subgraph G_s is not statically defined but is dynamically constructed through a MoE mechanism. Rather than selecting a single predefined topology from the candidate set G_g as Figure 2 shows, which comprises subgraphs initialised using four sampling strategies, G_s is instead formed as a weighted combination of these alternatives. The MoE gating function $G(h_i)$ adaptively assigns importance to each subgraph, enabling task-aware, localised modelling while preserving structural diversity and alignment with global graph semantics.

The MoE adaptively selects subgraph topologies by learning an optimal weighting scheme $G(h_i)$ to minimize JS divergence. This ensures subgraph representations align with the global graph's structure and attributes, effectively retaining local and global information to enhance POI embedding robustness and expressiveness.

4.5 Encoder-Decoder Structure

Ultimately, within the Encoder-Decoder architecture, an MLP-based decoder is utilized to interpret and extract latent representation provided by the adaptive representation learning module.

4.5.1 Decoder We utilize three distinct MLPs as FFN_{txt} , FFN_{geo} and FFN_{occ} for decoding the Co-occurrence representation, Geographical representation, and Mixed user text representation [24].

Inspired by BERT in the NLP models, we implement the Masked Language Model (MLM) to construct the self-supervised learning fashion in the training phase. As figure 2 shows, we randomly mask 20% records of $X_{p_i}^{txt}$, $S_{p_i}^{txt}$ and replace the corresponding text with special token $[X_{p_i}^{txt}]_m$, $[S_{p_i}^{txt}]_m$ respectively. Therefore, the $[e_{i,n}^{occ}]_m$, $[e_{i,n}^{geo}]_m$ will be represented accordingly by GOT representation following 4.2. Let f be the mapping function in the encoder, and we aim to predict the masked token formulated by:

$$\begin{aligned} \hat{X}_{p_i}^{txt} &= FFN_{txt}(f([X_{p_i}^{txt}]_m)) & \hat{e}_{i,n}^{occ} &= FFN_{occ}(f([e_{i,n}^{occ}]_m)) \\ \hat{e}_{i,n}^{geo} &= FFN_{geo}(f([e_{i,n}^{geo}]_m)) \end{aligned} \quad (24)$$

4.5.2 Loss Function As our methodology is designed to be task-agnostic, emphasizing the acquisition of general representations applicable across diverse applications, the loss function is tailored not for task-specific objectives but rather for reconstructing or closely approximating the original input information, spanning text, spatial, and co-occurrence data. Therefore, we utilize a weighted loss strategy:

Textual Loss (L_{txt}) measures the discrepancy between predicted and true text features, using binary cross-entropy for one-hot encoded text data:

$$L_i^{txt} = \text{CrossEntropy}(\hat{X}_{p_i}^{txt}, X_i^{txt}) \quad (25)$$

Geographical Loss (L_{geo}) gauges the discrepancy in predicting spatial features (distance and azimuth) between pairs of Points of Interest (POIs), utilizing mean squared error (MSE):

$$L_{ij}^{geo} = \text{MSE}(\hat{e}_{i,n}^{geo}, e_{ij}^{geo}) \quad (26)$$

Co-occurrence Loss (L_{occ}) assesses the error, i.e., MSE, in predicting the frequency of co-occurrence between POI pairs:

$$L_{ij}^{occ} = \text{MSE}(\hat{e}_{i,n}^{occ}, e_{ij}^{occ}) \quad (27)$$

MOE Loss To address the imbalance caused by certain experts being over-selected due to self-reinforcement, we introduce an importance loss mechanism to balance multiple contexts [32, 35]:

$$\text{Imp}(H) = \sum_{h_i \in H, g \in G(h_i)} g, \quad L_{\text{imp}}(H) = \text{CV}(\text{Imp}(H))^2, \quad (28)$$

where $\text{Imp}(H)$ is the sum of each node's gate value g across the batch, and CV is the coefficient of variation. This importance loss $L_{\text{imp}}(H)$ ensures balanced expert selection. Additionally, JS divergence serves as an auxiliary loss during training.

Overall Loss To allow the model to automatically balance multiple objectives, we define the overall loss (L_{total}) as a softmax-normalised weighted sum of individual loss components:

$$L_{\text{total}} = \sum_k \alpha_k L_k, \quad \text{where} \quad \alpha_k = \frac{\exp(w_k)}{\sum_j \exp(w_j)} \quad (29)$$

Here, $\{w_k\}$ denotes a set of learnable scalar parameters associated with each loss component $L_k \in \{L_{\text{txt}}, L_{\text{geo}}, L_{\text{occ}}, L_{\text{imp}}, L_{\text{JS}}\}$. This learnable weighting scheme allows the model to dynamically adapt the contribution of each context during training process.

Time complexity The time complexity can be represented as: $O(k \sum_{h_i \in H} \sum_{j \in N_i} (|V|FF' + |E|F'))$, where the right part represents the time complexity from attention[34], where F, F' is the number of input features and output features, $|V|$ and $|E|$ represent the number of nodes and edges respectively. The left part denotes the time complexity of fusing o experts, similar as [35], the h_i denotes the input feature of i -th node, j denotes the j -th node; H and N_i denote the number of input feature dimension and neighborhood of i -th node respectively.

5 Experiments

5.1 EXPERIMENTAL SETUP

Table 1: Statistics of Datasets

Dataset	#Category	City/State	#User	#POI	#Check-in
Foursquare	9	New York	1,083	9,989	179,468
		Tokyo	2,293	15,177	494,807
Yelp	21	Louisiana	40,183	7,811	106,469
		Nevada	18,573	5,317	53,053

5.1.1 Datasets **Foursquare**² comprises check-in data from two major cities, New York (NY) and Tokyo City, spanning from April 2012 to February 2013. Each check-in entry includes geographical coordinates, timestamps, and the category of the visited POI. **Yelp**³ is a subset of Yelp’s businesses, reviews, and users’ check-in data. We narrowed down the dataset to focus on information from the states of Nevada (NV) and Louisiana (LA).

5.1.2 Evaluation Metrics We calculate two widely used measure in recommender systems: Recall@K metric and NDCG@K [17], we only show Recall@K by simplicity on this paper⁴. They signify the proportion of relevant items within the top K items compared to all relevant items:

5.1.3 Baseline The baselines of pre-trained embedding models: **FC**: fully connected model. **Rand**: Random initialization. **CTLE** [24]: A pre-trained method considering contextual neighbors within trajectories. The baselines of next POI and next category recommendation: **GETNEXT** [41], **FPMC** [31], **SERM** [42], **HSTLSTM** [19], **LSTPM** [33]. The baselines for POI Recommendation: **EEDN** [36] **VanillaMF** [20] **RankNet** [1] **NGCF** [37] **NeuMF** [14].

5.1.4 Implementation Details The number of heads A is set to 2 in AdaptGOT, neighbors k is set to 5, layer normalization epsilon (ϵ) is set to $1e-12$, the encoder dimensions d_k is 16 and a dropout probability (p) is set of 0.1. We use Adam optimizer[18] with a learning rate (l_r) of 0.001 and epoch of 100. For SpaBERT [22], the

²<https://sites.google.com/site/yangdingqi/home/foursquare-dataset>

³<https://www.kaggle.com/datasets/yelp-dataset/yelp-dataset>

⁴Extensive experiments on NDCG@k: <https://anonymous.4open.science/r/POIemb-F161/README>.

distance factor Z is 0.0001, and the distance separator D_{SEP} is set to 20. The embedding size d_{model} is set to 768.

The hyper-parameter is tuned following the grid search, For AdaptGOT: $A \in [1, 2, 4]$, $k \in [1 : 5]$, $d_k \in [4, 8, 16, 32]$; For others: $Z \in [0.001, 0.0001, 0.00001]$, $d_{model} \in [256, 512, 768]$. Our experiments were conducted on an AMD Ryzen 7 7700X CPU, 64GB RAM and an NVIDIA RTX 4090 GPU.

5.2 Overall Comparison

We report the results on three downstream tasks in Table 2.

5.2.1 Next POI Recommendation The table demonstrates GOT’s consistent superiority over baseline models, excelling in synthesizing contextual and sequential information for next POI recommendations. AdaptGOT achieves the highest recall scores, particularly in dense, multi-context environments like New York, where it improves Rec@5 by 23.8% over SpaBERT under FPMC and 15.5% under GETNEXT. In Los Angeles, GOT shows a 48.3% Rec@5 improvement over CTLE under FPMC and 36.5% over SpaBERT. AdaptGOT also leads in tasks like LSTPM and HST, achieving substantial gains such as 33.3% in Rec@10 over CTLE under LSTPM. In contrast, models like SpaBERT and CTLE fall short in capturing fine-grained contextual information.

5.2.2 Next Category Prediction GOT shows significant improvements over SpaBERT and CTLE across all models and metrics, particularly in the NY-Next dataset. In FPMC, it improves Rec@5 by 15.9% over SpaBERT and 9.8% over CTLE, highlighting its ability to synthesise context and check-in sequences. In GETNEXT on the LA dataset, GOT achieves 4.0% and 2.7% higher Rec@5 over CTLE and SpaBERT, respectively. These results underscore AdaptGOT’s strong contextual integration, especially in NY and LA.

5.2.3 POI Recommendation AdaptGOT outperforms baselines in POI recommendation. In New York, it improves Rec@5 by 16.7% and Rec@15 by 20.8% under FPMC compared to CTLE and achieves a 13.3% higher Rec@5 in GETNEXT over SpaBERT. In LA, it shows a 44.5% gain in Rec@5 over SpaBERT and a 14.3% improvement in Rec@15 compared to CTLE under FPMC. AdaptGOT also achieves notable gains in Rec@5, including 14.6% over SpaBERT under LSTPM and 15.4% over CTLE under HST, highlighting its superior ability to integrate multiple contexts for accurate POI predictions.

5.3 Ablation Studies

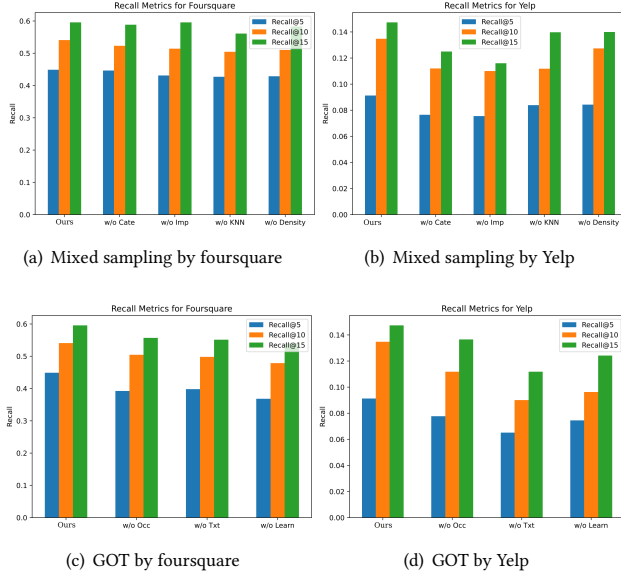
5.3.1 Sampling and GOT representation To evaluate the influence of each component within our representation on model performance, we conducted experiments on the next POI recommendation task using SERM [42] in the Foursquare (NY) dataset. Here are the experimental settings:

- w/o Cate, Imp, KNN and Density: it removes the category-aware sampling, importance sampling, KNN sampling, and density-based sampling respectively;
- w/o Occ, Txt, and Learn: it removes the co-occurrence representation and the text representation and freezes the POI embedding learning in the downstream training phase.

Figure 3 highlights the indispensability of each component in the mixed sampling and GOT frameworks. Removing any element reduces recall at @5, @10, and @15. In Figure 3 (a), excluding

Table 2: Overall comparison between AdaptGOT (GOT) and other pre-training model (PM) on three downstream models (DM).

Dataset and tasks		NY-Next POI rec			LA-Next POI rec			NY-Next cate rec			LA-Next cate rec			Baseline	NY-POI rec			LA-POI rec		
DM	PM	Rec@5	Rec@10	Rec@15	Rec@5	Rec@10	Rec@15	Rec@5	Rec@10	Rec@15	Rec@5	Rec@10	Rec@15	DM	Rec@5	Rec@10	Rec@15	Rec@5	Rec@10	Rec@15
FPMC	Rand	0.283	0.394	0.461	0.072	0.087	0.101	0.669	0.820	0.890	0.536	0.739	0.831	VaMF	0.104	0.175	0.257	0.143	0.196	0.234
	FC	0.277	0.382	0.446	0.067	0.082	0.089	0.678	0.857	0.911	0.548	0.755	0.842		0.107	0.179	0.262	0.151	0.207	0.238
	CTLE	0.252	0.364	0.431	0.058	0.076	0.078	0.668	0.826	0.855	0.541	0.722	0.837		0.112	0.173	0.257	0.146	0.198	0.232
	Spa	0.245	0.347	0.405	0.043	0.063	0.063	0.613	0.771	0.857	0.531	0.763	0.845		0.096	0.169	0.252	0.108	0.130	0.141
	GOT	0.312	0.423	0.486	0.086	0.125	0.156	0.711	0.862	0.927	0.605	0.794	0.885		0.121	0.186	0.273	0.163	0.224	0.269
LSTPM	Rand	0.399	0.485	0.529	0.064	0.079	0.089	0.759	0.874	0.928	0.639	0.782	0.866	RkNet	0.089	0.143	0.201	0.175	0.225	0.260
	FC	0.386	0.473	0.521	0.058	0.071	0.075	0.747	0.853	0.915	0.618	0.753	0.847		0.092	0.147	0.208	0.182	0.231	0.268
	CTLE	0.388	0.476	0.525	0.063	0.075	0.079	0.756	0.874	0.914	0.559	0.736	0.789		0.097	0.157	0.219	0.178	0.237	0.269
	Spa	0.395	0.483	0.528	0.078	0.084	0.089	0.759	0.883	0.929	0.564	0.743	0.802		0.092	0.149	0.212	0.173	0.229	0.260
	GOT	0.426	0.513	0.557	0.078	0.112	0.121	0.789	0.913	0.957	0.662	0.824	0.884		0.109	0.187	0.249	0.175	0.229	0.263
HST	Rand	0.327	0.392	0.428	0.033	0.059	0.069	0.705	0.840	0.901	0.580	0.715	0.784	NGCF	0.095	0.175	0.239	0.128	0.205	0.248
	FC	0.339	0.407	0.415	0.038	0.044	0.047	0.701	0.827	0.896	0.568	0.707	0.776		0.097	0.173	0.237	0.125	0.201	0.243
	CTLE	0.315	0.384	0.418	0.057	0.079	0.083	0.708	0.836	0.905	0.577	0.713	0.784		0.094	0.178	0.231	0.117	0.198	0.245
	Spa	0.309	0.376	0.411	0.051	0.071	0.076	0.699	0.838	0.899	0.557	0.814	0.880		0.111	0.170	0.242	0.153	0.213	0.262
	GOT	0.358	0.431	0.470	0.048	0.071	0.087	0.724	0.849	0.904	0.606	0.748	0.791		0.093	0.187	0.254	0.147	0.201	0.259
SERM	Rand	0.397	0.495	0.544	0.062	0.078	0.102	0.727	0.852	0.907	0.581	0.776	0.882	NeuMF	0.101	0.166	0.254	0.142	0.208	0.254
	FC	0.394	0.489	0.538	0.057	0.072	0.094	0.732	0.859	0.912	0.592	0.792	0.831		0.093	0.153	0.238	0.128	0.185	0.241
	CTLE	0.394	0.492	0.544	0.061	0.092	0.112	0.738	0.862	0.917	0.599	0.788	0.844		0.091	0.148	0.234	0.122	0.178	0.233
	Spa	0.399	0.495	0.551	0.065	0.096	0.121	0.754	0.877	0.926	0.624	0.811	0.857		0.095	0.179	0.233	0.153	0.203	0.250
	GOT	0.427	0.523	0.561	0.084	0.112	0.140	0.758	0.880	0.928	0.603	0.817	0.873		0.095	0.180	0.255	0.153	0.209	0.256
GETNEXT	Rand	0.416	0.508	0.554	0.079	0.104	0.128	0.747	0.865	0.903	0.592	0.794	0.850	EEDN	0.117	0.179	0.268	0.158	0.217	0.268
	FC	0.423	0.513	0.561	0.082	0.108	0.135	0.752	0.871	0.912	0.607	0.788	0.839		0.119	0.183	0.271	0.166	0.228	0.271
	CTLE	0.432	0.525	0.564	0.088	0.115	0.139	0.763	0.878	0.916	0.623	0.811	0.845		0.126	0.190	0.277	0.165	0.231	0.277
	Spa	0.441	0.527	0.589	0.096	0.119	0.143	0.771	0.886	0.932	0.631	0.827	0.864		0.135	0.195	0.293	0.171	0.235	0.286
	GOT	0.447	0.536	0.593	0.102	0.126	0.152	0.775	0.894	0.946	0.648	0.835	0.892		0.143	0.196	0.297	0.177	0.246	0.293

**Figure 3: Ablation study on mixed sampling and GOT representation.**

density-based sampling or KNN lowers Recall@5 by 7.6% and 7.7%, while removing category-aware or importance sampling reduces Recall@10 by 3.3% and 5.0%. Figure 3 (b) shows average recall drops of 19.0% and 10.1% without category-aware or importance sampling.

Figure 3 (c) reveals that removing co-occurrence, text representation, or all components reduces Recall@5 by 12.6%, 11.2%, and 17.9%, respectively, while freezing embeddings causes the largest drop. In Figure 3 (d), omitting text encoding cuts average recall by 28.6%. These results highlight the critical role of multi-contextual and text information in POI embeddings.

5.3.2 Adaptive module and Attention mechanism We show the ablation study on adaptive and attention module by Table 3. Specifically, we remove the component with the adaptive representation

Table 3: Ablation study on Adaptive Representation Aggregator (ARA) and attention mechanism.

Dataset		NY-Next POI rec			LA-Next POI rec		
DM	PM	Rec@5	Rec@10	Rec@15	Rec@5	Rec@10	Rec@15
FPMC	GOTAtt	0.278	0.389	0.448	0.062	0.103	0.127
	w/o ARA	0.275	0.384	0.441	0.06	0.098	0.123
	w/o G	0.284	0.401	0.463	0.068	0.111	0.134
	w/o O	0.295	0.408	0.468	0.073	0.118	0.141
	GOT	0.312	0.423	0.486	0.086	0.125	0.156
LSTPM	GOTAtt	0.396	0.492	0.526	0.061	0.095	0.103
	w/o ARA	0.392	0.487	0.519	0.058	0.095	0.102
	w/o G	0.411	0.504	0.539	0.071	0.103	0.114
	w/o O	0.415	0.511	0.546	0.073	0.107	0.116
	GOT	0.426	0.513	0.557	0.078	0.112	0.121

aggregator by w/o ARA, Geographical component by w/o G, the Co-occurrence component by w/o O, and the Textual component by w/o T. We also replace GOTAtt with Vanilla Attention by GOTAtt.

The results first demonstrate the critical role of the adaptive component. Removing ARA (w/o ARA) consistently leads to performance degradation across both datasets and baselines, underscoring its importance in adaptively aggregating subgraphs. In addition, the effectiveness of the proposed GOT attention mechanism is clearly validated by comparisons with its ablated variants (GOTAtt, w/o G, w/o O, and w/o T). GOT consistently outperforms these alternatives in terms of recall. Notably, under the FPMC model on the NY dataset, GOT achieves a 12.2% improvement in Recall@5 (from 0.278 to 0.312) and an 8.5% gain in Recall@15 (from 0.448 to 0.486), further confirming the value of GOT attention mechanism.

5.4 Case Studies

This case study addresses two questions: 1) Can AdaptGOT learn related subgraphs through mixed sampling? 2) Can AdaptGOT identify GOT contexts? Using 100 randomly selected POIs from the Yelp dataset as Figure 4 (a) shows, we analysed subgraphs and embeddings. Figure 4 (b) shows BNS-generated subgraphs [43], which

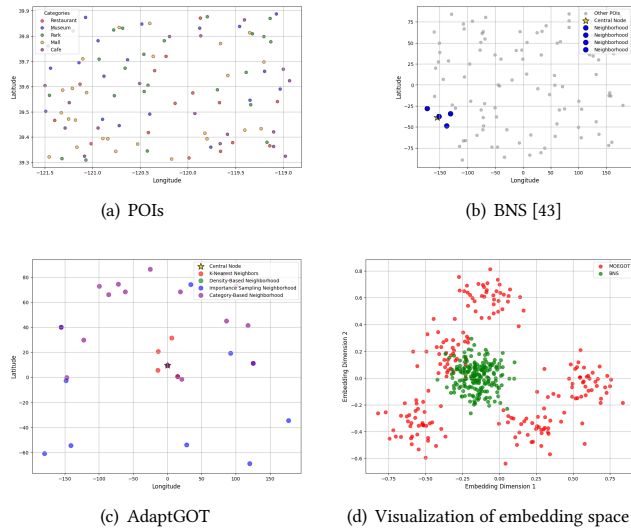


Figure 4: Case study on the Yelp dataset. Each subfigure represents key insights about POI selection, neighborhood generation, and embedding space exploration.

focus on proximal neighbors but ignore broader contextual factors. In contrast, Figure 4 (c) highlights AdaptGOT’s ability to integrate category, density, and proximity, creating robust subgraphs. Figure 4 (d) compares embedding spaces, where AdaptGOT produces globally uniform embeddings that absorb diverse contexts, while BNS suffers from over-smoothing and clustered representations. Overall, AdaptGOT effectively captures contextual information, outperforming BNS in subgraph and embedding quality.

5.5 Sensitivity Studies

In this section, we study the impact of parameters for AdaptGOT on the next POI recommendation task and use recall, F1 score, Mean Reciprocal Rank (MRR), and Normalized Discounted Cumulative Gain (NDCG) as performance metrics.

5.5.1 Number of subgraphs We evaluated subgraphs ranging from 2 to 6, using random combinations of sampling methods for two or three subgraphs⁵. Performance peaked with four subgraphs, offering the best balance of effectiveness and computational efficiency in Table 4. While additional subgraphs slightly improved performance, the gains were marginal and incurred higher computational costs. Therefore, we chose four subgraphs as optimal for both datasets.

Table 4: Sensitivity to the number of subgraphs in FPMC [31] for next POI recommendation.

Dataset	Rec@5	Rec@10	Rec@15	Rec@5	Rec@10	Rec@15	
DM	Num	NY-Next POI rec			LA-Next POI rec		
FPMC	2	0.298	0.411	0.472	0.073	0.107	0.142
	3	0.307	0.418	0.479	0.081	0.118	0.149
	4	0.312	0.423	0.486	0.086	0.125	0.156
	5	0.313	0.426	0.483	0.085	0.123	0.154
	6	0.312	0.423	0.483	0.087	0.124	0.155

⁵We claim that when the number of subgraphs above 4, additional subgraph structures are constructed by different parameters (e.g. different k in KNN) to prevent the over-reliance on redundant topologies.

5.5.2 Number of Neighbours Connections To examine the impact of varying the number of neighbour connections during the graph construction phase in pre-training on downstream task performance, we employ the HST-LSTM for the next POI recommendation task on Yelp LA with the number of neighbours of 5, 10 and 15. As figure 5 shows, 15 neighborhoods outperform others in the majority cases.

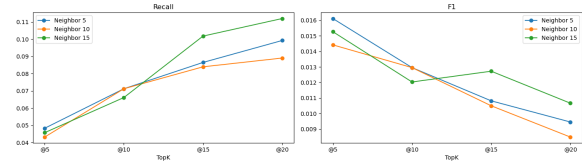


Figure 5: Sensitivity studies on different number of neighbours connection.

5.5.3 Number of heads in GOT Attention In the GOT Attention mechanism, we assess the impact of varying the number of heads in multi-head attention by selecting 1, 2, or 4 heads. We employ the HST-LSTM model [19] as the downstream model for the next POI recommendation task. As depicted in Figure 6, the configuration with 2 heads demonstrates superior performance.

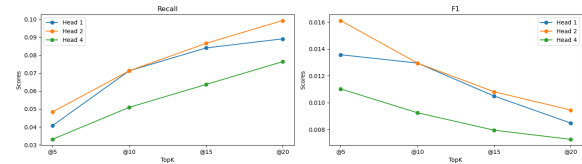


Figure 6: Sensitivity study on different heads numbers.

5.6 Zero-shot Cross-city Generalisation

We evaluated the cross-city transferability of AdaptGOT using Foursquare and Yelp datasets. Table 5 highlights AdaptGOT’s superior performance, achieving an average recall increase of 19.7% and outperforming Random and SpaBERT embeddings on the Yelp LA dataset, with 14.9% and 20.1% improvements in Recall@5 and Recall@10, respectively.

Table 5: Cross-City Transferability Performance on Next POI Recommendation.

Dataset	DM	PM	Foursquare			Yelp		
			Rec@5	Rec@10	Rec@15	Rec@5	Rec@10	Rec@15
FPMC	Rand		0.283	0.394	0.461	0.072	0.087	0.101
FPMC	FC		0.275	0.388	0.437	0.059	0.074	0.087
FPMC	CTLE		0.286	0.401	0.464	0.075	0.096	0.115
FPMC	Spa		0.242	0.340	0.397	0.034	0.058	0.073
FPMC	GOT		0.293	0.414	0.488	0.082	0.111	0.130
LSTPM	Rand		0.399	0.485	0.529	0.064	0.079	0.089
LSTPM	FC		0.394	0.490	0.533	0.069	0.084	0.092
LSTPM	CTLE		0.395	0.471	0.504	0.059	0.064	0.078
LSTPM	Spa		0.399	0.479	0.519	0.045	0.069	0.084
LSTPM	GOT		0.408	0.497	0.548	0.075	0.089	0.097

6 Conclusion

We presented AdaptGOT, a novel framework addressing key challenges in POI representation learning, such as multi-context sampling strategies, insufficient exploration of multiple POI contexts, and limited adaptability to diverse tasks. By integrating an adaptive learning component with Geographical-Co-Occurrence-Text (GOT) representations, AdaptGOT enhances the expressive power and versatility of POI embeddings. Extensive experiments demonstrated the superior performance of AdaptGOT compared to state-of-the-art POI embedding methods.

References

- [1] Chris Burges, Tal Shaked, Erin Renshaw, Ari Lazier, Matt Deeds, Nicole Hamilton, and Greg Hullender. 2005. Learning to rank using gradient descent. In *Proceedings of the 22nd international conference on Machine Learning*. 89–96.
- [2] Buru Chang, Yonggyu Park, Donghyeon Park, Seongsoo Kim, and Jaewoo Kang. 2018. Content-Aware Hierarchical Point-of-Interest Embedding Model for Successive POI Recommendation. In *Proceedings of the 27th International Joint Conference on Artificial Intelligence (Stockholm, Sweden) (IJCAI'18)*. AAAI Press, 3301–3307.
- [3] Jie Chen, Tengfei Ma, and Cao Xiao. 2018. FastGCN: Fast Learning with Graph Convolutional Networks via Importance Sampling. (1 2018). <http://arxiv.org/abs/1801.10247>
- [4] Jianfei Chen, Jun Zhu, and Le Song. 2017. Stochastic training of graph convolutional networks with variance reduction. *arXiv preprint arXiv:1710.10568* (2017).
- [5] Meng Chen, Yan Zhao, Yang Liu, Xiaohui Yu, and Kai Zheng. 2020. Modeling spatial trajectories with attribute representation learning. *IEEE transactions on knowledge and data engineering* 34, 4 (2020), 1902–1914.
- [6] Meng Chen, Lei Zhu, Ronghui Xu, Yang Liu, Xiaohui Yu, and Yilong Yin. 2021. Embedding Hierarchical Structures for Venue Category Representation. *ACM Trans. Inf. Syst.* 40, 3, Article 57 (nov 2021), 29 pages. doi:10.1145/3478285
- [7] Wei-Lin Chiang, Xuanqing Liu, Si Si, Yang Li, Samy Bengio, and Cho-Jui Hsieh. 2019. Cluster-gcn: An efficient algorithm for training deep and large graph convolutional networks. In *Proceedings of the 25th ACM SIGKDD international conference on knowledge discovery & data mining*. 257–266.
- [8] Weilin Cong, Rana Forsati, Mahmut Kandemir, and Mehrdad Mahdavi. 2020. Minimal variance sampling with provable guarantees for fast training of graph neural networks. In *Proceedings of the 26th ACM SIGKDD International Conference on Knowledge Discovery & Data Mining*. 1393–1403.
- [9] Yue Cui, Hao Sun, Yan Zhao, Hongzhi Yin, and Kai Zheng. 2021. Sequential-Knowledge-Aware Next POI Recommendation: A Meta-Learning Approach. *ACM Trans. Inf. Syst.* 40, 2, Article 23 (sep 2021), 22 pages. doi:10.1145/3460198
- [10] Jacob Devlin, Ming-Wei Chang, Kenton Lee, and Kristina Toutanova. 2018. BERT: Pre-training of Deep Bidirectional Transformers for Language Understanding. *CoRR* abs/1810.04805 (2018). arXiv:1810.04805 <http://arxiv.org/abs/1810.04805>
- [11] Ruixue Ding, Boli Chen, Pengjun Xie, Fei Huang, Xin Li, Qiang Zhang, and Yao Xu. 2023. A Multi-Modal Geographic Pre-Training Method. *arXiv preprint arXiv:2301.04283* (2023).
- [12] Shanshan Feng, Gao Cong, Bo An, and Yeow Meng Chee. 2017. Poi2vec: Geographical latent representation for predicting future visitors. In *Proceedings of the AAAI Conference on Artificial Intelligence*, Vol. 31.
- [13] Martin L. Hazelton. 2014. *Kernel Smoothing*. Wiley StatsRef: Statistics Reference Online.
- [14] Xiangnan He, Lizi Liao, Hanwang Zhang, Liqiang Nie, Xia Hu, and Tat-Seng Chua. 2017. Neural collaborative filtering. In *Proceedings of the 26th international conference on world wide web*. 173–182.
- [15] Wenbing Huang, Tong Zhang, Yu Rong, and Junzhou Huang. 2018. Adaptive sampling towards fast graph representation learning. *Advances in neural information processing systems* 31 (2018).
- [16] Yannis Karmim, Elias Ramzi, Raphaël Fournier-S'niehotta, and Nicolas Thome. 2024. ITEM: Improving Training and Evaluation of Message-Passing based GNNs for top-k recommendation. *Trans. Mach. Learn. Res.* 2024 (2024). <https://openreview.net/forum?id=9B6LM2uoEs>
- [17] Minseok Kim, Jinoh Oh, Jaeyoung Do, and Sungjin Lee. 2022. Debiasing Neighbor Aggregation for Graph Neural Network in Recommender Systems. *International Conference on Information and Knowledge Management, Proceedings*, 4128–4132.
- [18] Diederik P Kingma and Jimmy Ba. 2014. Adam: A method for stochastic optimization. *arXiv preprint arXiv:1412.6980* (2014).
- [19] Dejiang Kong and Fei Wu. 2018. HST-LSTM: A hierarchical spatial-temporal long-short term memory network for location prediction.. In *IJCAI*, Vol. 18. 2341–2347.
- [20] Yehuda Koren, Robert Bell, and Chris Volinsky. 2009. Matrix factorization techniques for recommender systems. *Computer* 42, 8 (2009), 30–37.
- [21] Yang Li, Yadan Luo, Zheng Zhang, Shazia Sadiq, and Peng Cui. 2019. Context-aware attention-based data augmentation for POI recommendation. In *2019 IEEE 35th International Conference on Data Engineering Workshops (ICDEW)*. IEEE, 177–184.
- [22] Zekun Li, Jina Kim, Yao-Yi Chiang, and Muhao Chen. 2022. SpaBERT: A Pre-trained Language Model from Geographic Data for Geo-Entity Representation. arXiv:2210.12213 [cs.CL]
- [23] Defu Lian, Yongji Wu, Yong Ge, Xing Xie, and Enhong Chen. 2020. Geography-aware sequential location recommendation. In *Proceedings of the 26th ACM SIGKDD international conference on knowledge discovery & data mining*. 2009–2019.
- [24] Yan Lin, Huaiyu Wan, Shengnan Guo, and Youfang Lin. 2021. Pre-training context and time aware location embeddings from spatial-temporal trajectories for user next location prediction. In *Proceedings of the AAAI Conference on Artificial Intelligence*, Vol. 35. 4241–4248.
- [25] Fan Liu, Zhiyong Cheng, Lei Zhu, Zan Gao, and Liqiang Nie. 2021. Interest-aware Message-Passing GCN for Recommendation. In *WWW '21: The Web Conference 2021, Virtual Event / Ljubljana, Slovenia, April 19-23, 2021*, Jure Leskovec, Marko Grobelnik, Marc Najork, Jie Tang, and Leila Zia (Eds.). ACM / IW3C2, 1296–1305. doi:10.1145/3442381.3449986
- [26] Xin Liu, Yong Liu, and Xiaoli Li. 2016. Exploring the context of locations for personalized location recommendations.. In *IJCAI*. 1188–1194.
- [27] Steven Loria et al. 2018. textblob Documentation. *Release 0.15.2*, 8 (2018), 269.
- [28] Saeed Masoudnia and Reza Ebrahimpour. 2014. Mixture of experts: a literature survey. *Artificial Intelligence Review* 42 (2014), 275–293.
- [29] Christopher Morris, Gaurav Rattan, and Petra Mutzel. 2020. Weisfeiler and Leman go sparse: Towards scalable higher-order graph embeddings. In *Advances in Neural Information Processing Systems 33: Annual Conference on Neural Information Processing Systems 2020, NeurIPS 2020, December 6-12, 2020, virtual*.
- [30] Christopher Morris, Martin Ritzert, Matthias Fey, William L Hamilton, Jan Eric Lenssen, Gaurav Rattan, and Martin Grohe. 2019. Weisfeiler and leman go neural: Higher-order graph neural networks. In *Proceedings of the AAAI conference on artificial intelligence*, Vol. 33. 4602–4609.
- [31] Steffen Rendle, Christoph Freudenthaler, and Lars Schmidt-Thieme. 2010. Factorizing personalized markov chains for next-basket recommendation. In *Proceedings of the 19th international conference on World wide web*. 811–820.
- [32] N Shazeer, A Mirhoseini, K Maziarz, A Davis, Q Le, G Hinton, and J Dean. 2017. The sparsely-gated mixture-of-experts layer. *Outrageously large neural networks* (2017).
- [33] Ke Sun, Tiejun Qian, Tong Chen, Yile Liang, Nguyen Hung, and Hongzhi Yin. 2020. Where to Go Next: Modeling Long- and Short-Term User Preferences for Point-of-Interest Recommendation. *Proceedings of the AAAI Conference on Artificial Intelligence* 34 (04 2020), 214–221. doi:10.1609/aaai.v34i01.5353
- [34] Petar Veličković, Guillem Cucurull, Arantxa Casanova, Adriana Romero, Pietro Lio, and Yoshua Bengio. 2017. Graph attention networks. *arXiv preprint arXiv:1710.10903* (2017).
- [35] Haotao Wang, Ziyu Jiang, Yuning You, Yan Han, Gaowen Liu, Jayanth Srinivasa, Ramana Rao Kompella, and Zhangyang Wang. 2023. Graph Mixture of Experts: Learning on Large-Scale Graphs with Explicit Diversity Modeling. (4 2023). <http://arxiv.org/abs/2304.02806>
- [36] Xinfeng Wang, Fumiyo Fukumoto, Jin Cui, Yoshimi Suzuki, Jiyi Li, and Dongjin Yu. 2023. EEDN: Enhanced Encoder-Decoder Network with Local and Global Context Learning for POI Recommendation. In *Proceedings of the 46th International ACM SIGIR Conference on Research and Development in Information Retrieval*. 383–392.
- [37] Xiang Wang, Xiangnan He, Meng Wang, Fuli Feng, and Tat-Seng Chua. 2019. Neural graph collaborative filtering. In *Proceedings of the 42nd international ACM SIGIR conference on Research and development in Information Retrieval*. 165–174.
- [38] Keyulu Xu, Weihua Hu, Jure Leskovec, and Stefanie Jegelka. 2019. How Powerful are Graph Neural Networks?. In *7th International Conference on Learning Representations, ICLR 2019, New Orleans, LA, USA, May 6-9, 2019*. OpenReview.net. <https://openreview.net/forum?id=ryGs6iA5Km>
- [39] Jingsong Yang, Guanzhou Han, Deqing Yang, Jingping Liu, Yanghua Xiao, Xiang Xu, Baohua Wu, and Shenghua Ni. 2023. M3pt: A multi-modal model for poi tagging. In *Proceedings of the 29th ACM SIGKDD Conference on Knowledge Discovery and Data Mining*. 5382–5392.
- [40] Kang Yang, Ruiyun Yu, Bingyang Guo, and Jie Li. 2024. Interaction Subgraph Sequential Topology-Aware Network for Transferable Recommendation. *IEEE Trans. Knowl. Data Eng.* 36, 10 (2024), 5221–5233. doi:10.1109/TKDE.2024.3384965
- [41] Song Yang, Jiamou Liu, and Kaiqi Zhao. 2022. GETNext: Trajectory Flow Map Enhanced Transformer for Next POI Recommendation. In *Proceedings of the 45th International ACM SIGIR Conference on Research and Development in Information Retrieval (<conf-loc>, <city>Madrid</city>, <country>Spain</country>, </conf-loc>)* (SIGIR '22). Association for Computing Machinery, New York, NY, USA, 1144–1153. doi:10.1145/3477495.3531983
- [42] Di Yao, Chao Zhang, Jianhui Huang, and Jingping Bi. 2017. Serm: A recurrent model for next location prediction in semantic trajectories. In *Proceedings of the*

- 2017 ACM on Conference on Information and Knowledge Management. 2411–2414.
- [43] Kai-Lang Yao and Wu-Jun Li. 2021. Blocking-based Neighbor Sampling for Large-scale Graph Neural Networks. <https://cs.nju.edu.cn/lwj/>.
- [44] Feiyu Yin, Yong Liu, Zhiqi Shen, Lisi Chen, Shuo Shang, and Peng Han. 2023. Next POI Recommendation with Dynamic Graph and Explicit Dependency. In *Thirty-Seventh AAAI Conference on Artificial Intelligence, AAAI 2023, Thirty-Fifth Conference on Innovative Applications of Artificial Intelligence, IAAI 2023, Thirteenth Symposium on Educational Advances in Artificial Intelligence, EAAI 2023, Washington, DC, USA, February 7–14, 2023*, Brian Williams, Yiling Chen, and Jennifer Neville (Eds.). AAAI Press, 4827–4834. doi:10.1609/AAAI.V37I4.25608
- [45] Hanqing Zeng, Hongkuan Zhou, Ajitesh Srivastava, Rajgopal Kannan, and Viktor Prasanna. 2019. Graphsaint: Graph sampling based inductive learning method. *arXiv preprint arXiv:1907.04931* (2019).
- [46] Hao Zhang, Siyi Wei, Xiaojiao Hu, Ying Li, and Jiajie Xu. 2020. On accurate POI recommendation via transfer learning. *Distributed and Parallel Databases* 38 (2020), 585–599.
- [47] Qianru Zhang, Lianghao Xia, Xuheng Cai, Siu-Ming Yiu, Chao Huang, and Christian S Jensen. 2024. Graph augmentation for recommendation. In *2024 IEEE 40th International Conference on Data Engineering (ICDE)*. IEEE, 557–569.
- [48] Zhenning Zhang, Boxin Du, and Hanghang Tong. 2022. SuGeR: A Subgraph-based Graph Convolutional Network Method for Bundle Recommendation. In *Proceedings of the 31st ACM International Conference on Information & Knowledge Management, Atlanta, GA, USA, October 17–21, 2022*, Mohammad Al Hasan and Li Xiong (Eds.). ACM, 4712–4716. doi:10.1145/3511808.3557707
- [49] Lingxiao Zhao, Wei Jin, Leman Akoglu, and Neil Shah. 2021. From stars to subgraphs: Uplifting any GNN with local structure awareness. *arXiv preprint arXiv:2110.03753* (2021).
- [50] Zhehan Zhao, Lu Bai, Lixin Cui, Ming Li, Yue Wang, Lixiang Xu, and Edwin R Hancock. 2024. ENADPool: The Edge-Node Attention-based Differentiable Pooling for Graph Neural Networks. *arXiv preprint arXiv:2405.10218* (2024).
- [51] Difan Zou, Ziniu Hu, Yewen Wang, Song Jiang, Yizhou Sun, and Quanquan Gu. 2019. Ladies: Layer-Dependent Importance Sampling for Training Deep and Large Graph Convolutional Networks. (11 2019).

Received 20 February 2007; revised 12 March 2009; accepted 5 June 2009